Journal of Financial Stability 81 (2025) 101477

Contents lists available at ScienceDirect

Journal of Financial Stability

journal homepage: www.elsevier.com/locate/jfstabil

A second-order finite difference method for the Black–Scholes model without far-field boundary conditions☆

Jian Wang [a], Lin Wu [a], Xinpei Wu [b], Youngjin Hwang [b], Yunjae Nam [c], Soobin Kwak [b], Taehui Lee [c], Junseok Kim [b,*]

[a] School of Mathematics and Statistics, Nanjing University of Information Science and Technology, Nanjing, 210044, China
[b] Department of Mathematics, Korea University, Seoul 02841, Republic of Korea
[c] Program in Actuarial Science and Financial Engineering, Korea University, Seoul, 02841, Republic of Korea

ARTICLE INFO

Keywords:
Second-order convergence
Finite difference method
Far-field boundary conditions

ABSTRACT

We propose an explicit finite difference method for the Black–Scholes (BS) equation that avoids artificial far-field boundary conditions. The method uses an alternating direction explicit (ADE) update on a dynamically shrinking grid, thereby eliminating the need for boundary values at the far end of the domain. It effectively alleviates the stability constraints of the explicit format through the alternating direction advancement. Numerical experiments on European and cash or nothing options confirm second-order convergence and demonstrate a high level of efficiency. For example, repeatedly doubling time resolution from 160 to 1280 reduces pricing error from 7.45×10^{-1} to 6.56×10^{-3}, with observed convergence rates close to 2. This makes the method suitable for low-latency financial applications such as real-time pricing and risk management.

1. Introduction

Options are derivative contracts that allow investors to buy or sell an underlying asset at a fixed price by a specified date for purposes of investment or risk management (Lyu et al., 2021; Sosa-Correa et al., 2018). Financial derivatives such as options can increase market efficiency, but they can also increase systemic risk. Option-based indicators have been used to predict macroeconomic conditions (Sill, 1997; Bevilacqua et al., 2023). Meanwhile, the positive impact of the use of derivatives on firms has been demonstrated in several papers. Derivatives can facilitate firms' investment financing by reducing information asymmetry. Furthermore, the option market helps to promote corporate innovation (Li, 2021; Blanco and Wehrheim, 2017; Cao et al., 2024). There are various models for option pricing, such as the binomial model (Benninga and Wiener, 1997; Tian, 1999; Shen and Pretorius, 2013), Monte Carlo simulation (Kim et al., 2024), and two-state models (Rendleman, 1979; Albanese et al., 2003). Mashayekhi and Mousavi (2022) proposed a finite difference scheme for single- and multi-asset European options that combines grid stretching near the strike with the antithetic Monte Carlo method at the domain boundaries. This scheme shows improved accuracy and reduced numerical error compared to standard finite difference and Monte Carlo approaches. Among these pricing methods, partial differential equation (PDE)-based models offer a powerful and flexible approach. These models can capture the continuous evolution of asset prices and are especially effective for deriving option values under various assumptions. One of the most influential PDE-based equations is the Black–Scholes (BS) model (Black and Scholes, 1973), which provides a foundation for modern option pricing theory and serves as a benchmark for evaluating numerical methods. Let $u(S,t)$ be the option value of the underlying asset S at time t. Numerous works (Engquist and Halpern, 1988; Gustafsson, 1988) have evolved its compatibility, so that the BS equation could be of greater use. In this paper, we consider the following BS equation:

$$\frac{\partial u(S,t)}{\partial t} = -\frac{1}{2}\sigma^2 S^2 \frac{\partial^2 u(S,t)}{\partial S^2} - rS\frac{\partial u(S,t)}{\partial S} + ru(S,t), \quad S > 0 \quad \text{and} \quad 0 \le t < T, \tag{1}$$

where σ denotes the asset's volatility, r represents the risk-free interest rate, and T indicates the time to maturity (Black and Scholes, 1973). The Black–Scholes equation models the evolution of option prices

☆ We would like to thank the anonymous referees for their valuable feedback and constructive suggestions, which have greatly improved the quality of this paper.

* Corresponding author.
E-mail addresses: 003328@nuist.edu.cn (J. Wang), 202412150819@nuist.edu.cn (L. Wu), xpwu012@korea.ac.kr (X. Wu), youngjin_hwang@korea.ac.kr (Y. Hwang), yjnam@korea.ac.kr (Y. Nam), soobin23@korea.ac.kr (S. Kwak), lth0407@korea.ac.kr (T. Lee), cfdkim@korea.ac.kr (J. Kim).
URL: https://mathematicians.korea.ac.kr/cfdkim/ (J. Kim).

https://doi.org/10.1016/j.jfs.2025.101477
Received 1 November 2024; Received in revised form 23 October 2025; Accepted 5 November 2025
Available online 13 November 2025

over time, typically defined on an unbounded spatial domain $S \in (0, \infty)$. To solve it numerically, most finite difference methods (FDMs) impose artificial far-field boundary conditions at a large but finite asset price $S_{\max}$. However, if $S_{\max}$ is not sufficiently large, or the boundary condition is not well designed, the resulting error may contaminate the solution in the region of interest, especially for long-dated or highly volatile options. This sensitivity is a major challenge when applying traditional schemes in practice.

In this paper, we introduce a novel computational algorithm for solving the BS model without imposing far-field boundary conditions. This scheme is rooted in the alternating direction explicit (ADE) method, renowned for its capability to accommodate large time steps while preserving numerical stability. Past works have shown its strength. Pourghanbar et al. (2020) analyze and demonstrate the efficiency and robustness of the unconditionally stable and explicit Saul'yev FDM for nonlinear partial differential equations. They also showed its superiority in elapsed time and closeness to the Crank–Nicolson method. Campbell and Yin (2007) developed and analyzed ADE finite-difference methods for time-dependent advection-diffusion equations. They identified stability limitations due to advection and proposing a stable scheme verified through quasi-linear one-dimensional problems. Buckova et al. (2015) investigated stability and consistency of ADE FDMs for convection–diffusion-reaction equations. They found that the average of two sweeps achieves a higher consistency of order $O(k^2 + h^2)$. Pealat and Duffy (2011) applied the ADE method to option pricing equations in one-factor models and showed its stability, accuracy, and suitability for uncertain volatility models and local volatility calibration, which makes it a preferable alternative to the Crank–Nicolson method.

To improve computational efficiency, we eliminate the need for far-field boundary conditions, which provides an innovative advantage. In this work, we adapt the ADE method specifically to the structure of the Black–Scholes equation by splitting the spatial operator and updating along alternating directions, followed by averaging. This enables explicit time integration while maintaining second-order accuracy and stability with relatively large time steps. Moreover, we incorporate a non-uniform spatial grid that is refined around the strike price, and coarsened in less sensitive regions. Unlike our work, past studies focused on applying far-field boundary conditions. Colonius and Taira (2008) developed a projection approach for the immersed boundary method with a multi-domain technique to improve far-field boundary conditions. Bayliss and Turkel (1982) derived a family of boundary conditions simulating outgoing radiation that significantly accelerates convergence to steady state in flow computations, with numerical results and potential extensions to duct geometries presented. Kangro and Nicolaides (2000) created pointwise error bounds for various boundary conditions on an artificial boundary in the numerical solution of European-style option pricing PDEs. These bounds enable one to determine a suitable boundary location in advance based on a given error tolerance. Svärd et al. (2007) constructed a stable high-order FDM for the compressible Navier–Stokes equations. They also demonstrated theoretical convergence rates, stability, and non-reflecting outflow conditions for various flow scenarios, including three-dimensional vortex shedding behind a circular cylinder.

Traditional numerical methods for solving the BS equation, such as finite difference and finite element schemes, often require the imposition of artificial far-field boundary conditions. These conditions can introduce significant approximation errors if the domain truncation is not carefully chosen.

In contrast, the proposed method eliminates the need for far-field boundary conditions by dynamically shrinking the computational domain. This not only simplifies the implementation but also improves numerical robustness by avoiding artificial reflections and boundary-induced errors. Beyond its numerical advantages, the proposed method has potential applicability in real-world financial computations where rapid and reliable option valuation is desired. By enabling large time steps and removing dependence on far-field boundary conditions, our method significantly improves computational speed and robustness.

The scope of this study is limited to one-dimensional Black–Scholes-type equations with European-style terminal payoff functions. The model assumes constant volatility and interest rates, and does not account for American-style early exercise features, stochastic volatility, or multiple underlying assets.

The contents of this paper are as follows: Section 2 presents a comprehensive description of the method used to approximate solutions of the BS equation. In Section 3, we present numerical tests, including applications to European call options and cash-or-nothing options, to demonstrate the second-order convergence and computational efficiency of our proposed method. Section 4 demonstrates that the proposed ADE-based no-boundary method achieves greater numerical stability and higher accuracy than the explicit Euler scheme. Finally, Section 5 concludes the paper.

2. Computational solution algorithm

Let $\tau = T - t$ and $x = S$. Then, Eq. (1) can be rewritten as

$$\frac{\partial u}{\partial \tau} = \frac{1}{2}(\sigma x)^2 \frac{\partial^2 u}{\partial x^2} + rx\frac{\partial u}{\partial x} - ru, \text{ for } x > 0,\ 0 < \tau \le T \tag{2}$$

with $u(x, 0)$ given in Dubey et al. (2019) and Farnoosh et al. (2016), which is discretized on a non-uniform grid (Hanh and Thanh, 2019; Lyu et al., 2021; Soleymani and Akgül, 2019). The non-uniform mesh is defined by $x_{i+1} = x_i + h_i$ for $i = 0, \dots, N_x - 1$, where $x_0 = 0$ and h_i denotes the spatial step size, and N_x is a positive integer of the total number of intervals, as displayed in Fig. 1.

Let $u_i^n = u(x_i, n\Delta\tau)$ for $n > 0$. Here, $\Delta\tau = T/N_\tau$ for some positive integer N_τ. We use the following discrete differential operators:

$$\left(\frac{\partial u}{\partial \tau}\right)_i^{n+1} = \frac{u_i^{n+1} - u_i^n}{\Delta\tau}, \tag{3}$$

$$\left(\frac{\partial u}{\partial x}\right)_i^{n+1} = \frac{h_{i-1}(u_{i+1}^{n+1} - u_i^{n+1})}{h_i(h_{i-1} + h_i)} + \frac{h_i(u_i^{n+1} - u_{i-1}^{n+1})}{h_{i-1}(h_{i-1} + h_i)}, \tag{4}$$

$$\left(\frac{\partial^2 u}{\partial x^2}\right)_i^{n+1} = \frac{u_{i+1}^{n+1} - u_i^{n+1}}{h_i(h_{i-1} + h_i)} - \frac{u_i^{n+1} - u_{i-1}^{n+1}}{h_{i-1}(h_{i-1} + h_i)}. \tag{5}$$

For the temporal discretization, a forward Euler method is applied, while second-order central differences are used for the spatial derivatives.

We set a spatial step size of 0.05, while for the time step we set different numbers of time nodes separately. These values are significantly larger than the time step normally allowed by explicit Eulerian methods under CFL conditions to demonstrate the advantages of the proposed method.

We apply the Saul'yev-type explicit scheme (Saul'Yev, 1964; Lee et al., 2023) to Eq. (2). Then, we use the technique that removes one end node position after each time step is updated. The process of calculating the numerical solution is described as follows. Let $u_i^0 = p_i$ for $i = 1, 2, \dots, N_x$, where p_i for $i = 1, 2, \dots, N_x$ are the initial conditions. Then, we consider the two sub-solutions ϕ_i^{n+1} and ψ_i^{n+1} for $n = 0, 1, 2, \dots, N_\tau - 1$ as follows:

For $i = 1, 2, \dots, N_x - n - 1$

$$\begin{aligned}\frac{\phi_i^{n+1} - u_i^n}{\Delta\tau} &= \sigma^2 x_i^2 \left(\frac{u_{i+1}^n - u_i^n}{h_i(h_{i-1} + h_i)} - \frac{\phi_i^{n+1} - \phi_{i-1}^{n+1}}{h_{i-1}(h_{i-1} + h_i)}\right) \\ &\quad + rx_i \left(\frac{h_{i-1}(u_{i+1}^n - u_i^n)}{h_i(h_{i-1} + h_i)} + \frac{h_i(\phi_i^{n+1} - \phi_{i-1}^{n+1})}{h_{i-1}(h_{i-1} + h_i)}\right) - \frac{r}{2}(u_i^n + \phi_i^{n+1}).\end{aligned} \tag{6}$$

For $i = N_x - n - 2, N_x - n - 3, \dots, 1$

$$\frac{\psi_i^{n+1} - u_i^n}{\Delta\tau} = \sigma^2 x_i^2 \left(\frac{\psi_{i+1}^{n+1} - \psi_i^{n+1}}{h_i(h_{i-1} + h_i)} - \frac{u_i^n - u_{i-1}^n}{h_{i-1}(h_{i-1} + h_i)}\right) \tag{7}$$

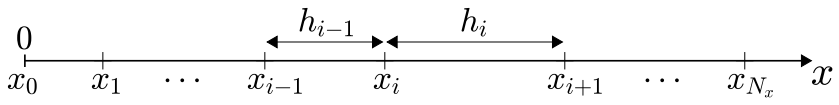

Fig. 1. Illustration of the discretized numerical domain.

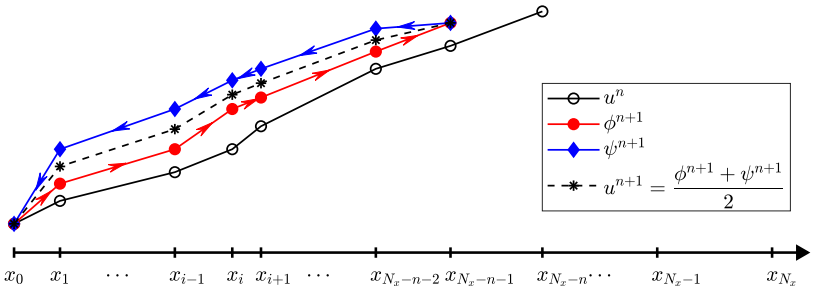

Fig. 2. Schematic of the proposed method.

$$+rx_i\left(\frac{h_{i-1}(\psi_{i+1}^{n+1}-\psi_i^{n+1})}{h_i(h_{i-1}+h_i)}+\frac{h_i(u_i^n-u_{i-1}^n)}{h_{i-1}(h_{i-1}+h_i)}\right)-\frac{r}{2}(u_i^n+\psi_i^{n+1}),$$

where $\psi_{N_x-n-1}^{n+1}=\phi_{N_x-n-1}^{n+1}$. Thus, Eqs. (6) and (7) can be rewritten in the explicit form for $n=0,1,\ldots,N_\tau-1$ as follows:

For $i=1,2,\ldots,N_x-n-1$

$$\phi_i^{n+1}=\left[\frac{u_i^n}{\Delta\tau}+\sigma^2x_i^2\left(\frac{u_{i+1}^n-u_i^n}{h_i(h_{i-1}+h_i)}+\frac{\phi_{i-1}^{n+1}}{h_{i-1}(h_{i-1}+h_i)}\right)\right.$$
$$\left.+rx_i\left(\frac{h_{i-1}(u_{i+1}^n-u_i^n)}{h_i(h_{i-1}+h_i)}-\frac{h_i\phi_{i-1}^{n+1}}{h_{i-1}(h_{i-1}+h_i)}\right)-\frac{r}{2}u_i^n\right]\Big/ f_i, \tag{8}$$

where $f_i=\frac{1}{\Delta\tau}+\frac{\sigma^2x_i^2-rx_ih_i}{h_{i-1}(h_{i-1}+h_i)}+\frac{r}{2}$.

For $i=N_x-n-2,N_x-n-3,\ldots,1$

$$\psi_i^{n+1}=\left[\frac{u_i^n}{\Delta\tau}+\sigma^2x_i^2\left(\frac{\psi_{i+1}^{n+1}}{h_i(h_{i-1}+h_i)}-\frac{u_i^n-u_{i-1}^n}{h_{i-1}(h_{i-1}+h_i)}\right)\right.$$
$$\left.+rx_i\left(\frac{h_{i-1}\psi_{i+1}^{n+1}}{h_i(h_{i-1}+h_i)}+\frac{h_i(u_i^n-u_{i-1}^n)}{h_{i-1}(h_{i-1}+h_i)}\right)-\frac{r}{2}u_i^n\right]\Big/ g_i, \tag{9}$$

where $g_i=\frac{1}{\Delta\tau}+\frac{\sigma^2x_i^2+rx_ih_{i-1}}{h_i(h_{i-1}+h_i)}+\frac{r}{2}$ and $\psi_{N_x-n-1}^{n+1}=\phi_{N_x-n-1}^{n+1}$.

Then, we compute the final solution u_i^{n+1} for $n=0,1,\ldots,N_\tau-1$ using the sub-solutions calculated by Eqs. (8) and (9) (see Fig. 2).

$$u_i^{n+1}=\frac{\phi_i^{n+1}+\psi_i^{n+1}}{2},\quad \text{for } i=1,\ldots,N_x-n-1. \tag{10}$$

At each time step, the final solution is computed as the average of two intermediate updates. This approach is rooted in Saul'yev-type alternating-direction methods and serves to eliminate directional bias and reduce numerical dispersion. The averaging step improves both stability and accuracy.

Unlike traditional explicit schemes such as the forward Euler method, which are subject to stringent stability conditions (e.g., CFL-type restrictions requiring $\Delta t \ll h^2$), the Saul'yev-type explicit method implemented here in the ADE methodology allows for significantly larger time steps while maintaining numerical stability. This is achieved by decomposing the spatial operator into two directional updates (forward and backward) and averaging their results at each time step.

In option pricing problems, the focus is on solutions near the current underlying asset price. For example, let $x_j=S_0$ and assume that we want to compute $u_{j-1}^{N_\tau}$, $u_j^{N_\tau}$, and $u_{j+1}^{N_\tau}$. Then, we define $N_x=N_\tau+j+1$; Thus, the computational solutions after N_τ time step iterations, $u_{j-1}^{N_\tau}$, $u_j^{N_\tau}$, and $u_{j+1}^{N_\tau}$, can be obtained. For pricing a European call option, the principal algorithm proceeds as follows: The value at the left boundary is fixed as $u_0^n=0$ for all n, and Eq. (8) is solved sequentially for $n=0,\ldots,N_\tau-1$ by progressively dropping the far-field boundary grid point after each time step update. Specifically, in the first time-step update, Eq. (8) is computed over the index range $i=1,\ldots,N_x-1$. In the second step, Eq. (8) is solved for $i=1,\ldots,N_x-2$, and this process continues until the final time step, where the equation is solved over $i=1,\ldots,j+1$. Consequently, the far-field boundary condition becomes unnecessary, as the grid is systematically reduced at each step (Jeong et al., 2018). Fig. 3 provides a schematic illustration of this grid reduction procedure.

Although referred to as a "non-uniform grid", our spatial mesh only deviates slightly from uniformity by setting the first and last grid intervals to half of the interior step size. This minor adjustment improves numerical symmetry near the boundaries and improves stability when handling payoff functions with discontinuities, such as cash-or-nothing options. The majority of the grid remains uniform, and thus standard second-order central difference formulas are used throughout without loss of accuracy.

3. Numerical tests

3.1. European call option

Let $u(x,0)=\max(x-K,0)$ on $\Omega=(0,4K)$ with $K=100$. Let $h=0.05$ and $\Omega_h=\{x_i|x_i=hi,\ \text{for } i=0,\ldots,4K/h\}$. Let T denote the total time to maturity of the option contract. We discretize the time domain into N_τ uniform intervals. The time-step size $\Delta\tau=T/N_\tau$ governs the temporal resolution of the numerical method and plays a critical role in ensuring both accuracy and stability. The parameters $r=0.03$, $\sigma=0.3$, and $T=0.1$ are adopted. The closed-form solution for the European call option (Feng et al., 2020) is given by

$$u(x,\tau)=xN(d_1)-Ke^{-r\tau}N(d_2), \tag{11}$$

where $d_1=\left(\ln(x/K)+\left(r+0.5\sigma^2\right)\tau\right)/(\sigma\sqrt{\tau})$, $d_2=d_1-\sigma\sqrt{\tau}$, and $N(d)$ denotes the cumulative distribution function (Black and Scholes, 1973; Ma et al., 2019):

$$N(d)=\frac{1}{\sqrt{2\pi}}\int_{-\infty}^{d}e^{-\frac{x^2}{2}}\mathrm{d}x. \tag{12}$$

We calculate the prices of European call options corresponding to underlying assets x and τ, and we select some data to display in Fig. 4, where $N_\tau=1280$. We can observe that as τ increases, the far-field boundary on the right side of the x-axis continues to shrink, dynamically reducing the computational domain from the right end. The final option prices are the values at $\tau=0.1$.

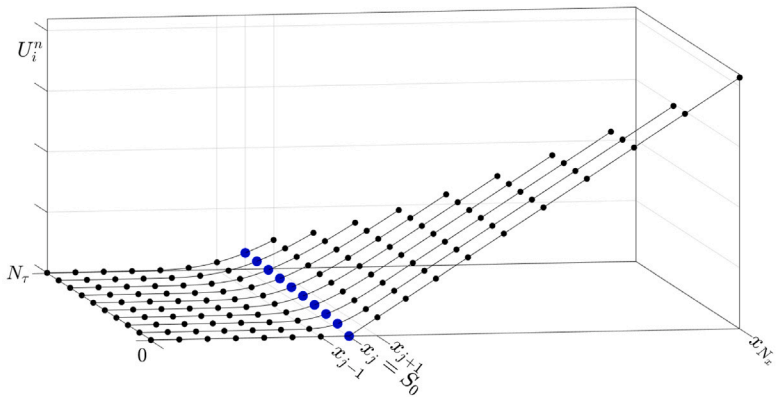

Fig. 3. Schematic of the reducing grids.

Table 1
Prices, errors, and convergence rates for the European call option at $x = 100$ with parameters $r = 0.03$, $\sigma = 0.3$, and $T = 0.1$. The exact value is 3.9123.

N_τ	160		320		640		1280
Price	3.1676		3.7501		3.8871		3.9189
Error	7.4467e−1		1.6218e−1		2.5169e−2		6.5586e−3
Convergence rate		2.20		2.69		1.94	

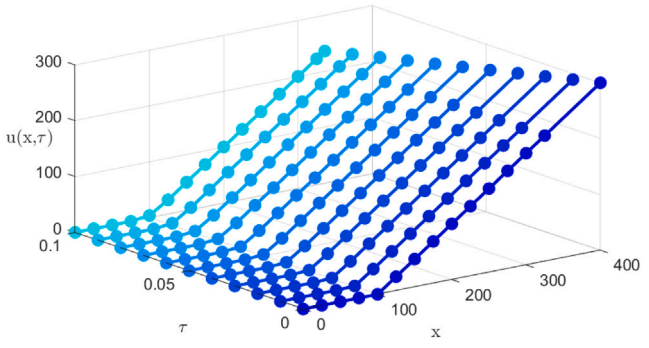

Fig. 4. Numerical results corresponding to the underlying asset and the time, here $N_\tau = 1280$ is adopted.

In addition, we compare the final option price with the accurate value of the analytical solution, as shown in Fig. 5(a), and the results indicate that the option price calculated by our proposed method was almost consistent with the analytical solution. To further validate the effectiveness and robustness of the method without far-field boundary conditions, we calculate and compare the numerical and analytical solutions of two Greeks Δ and Γ, as displayed in Fig. 5(b) and (c). The numerical schemes of Greeks Δ and Γ can be defined by

$$\Delta \approx \frac{u_{i+1}^n - u_{i-1}^n}{2h}, \tag{13}$$

$$\Gamma \approx \frac{u_{i+1}^n - 2u_i^n - u_{i-1}^n}{h^2}. \tag{14}$$

Besides, the exact results for the Greeks Δ and Γ are $\Delta = N(d_1)$ and $\Gamma = \frac{N'(d_1)}{x\sigma\sqrt{\tau}}$, respectively. We observe that the numerical results of the selected Greeks show uniformity with their analytic solutions. Table 1 shows the option prices, errors, and convergence rates of the European call option at $x = 100$. The error is calculated as $e_h^{N_\tau} = |u(100, T) - u_{100/h}^{N_\tau}|$. The convergence rate is defined as $\log_2\left(e_h^{N_\tau}/e_h^{2N_\tau}\right)$.

3.2. Cash or nothing option

In this section, we consider the cash or nothing option. The initial condition on domain $\Omega = (0, 4K)$ is given by

$$u(x,0) = \begin{cases} 0 & \text{if } x \le K, \\ C & \text{if } x > K. \end{cases}$$

The parameters are given as follows: $K = 100$, $\sigma = 0.3$, $r = 0.03$, $C = 100$, $T = 0.1$, $h = 0.05$, $N_x = 4K/h + 2$. We define the discrete domain $\Omega_h = \{x_i | x_0 = 0,\ x_i = (i-0.5)h,\ \text{for } i = 1, 2, \ldots, N_x - 1,\ x_{N_x} = 4K\}$. The analytic solution of the cash or nothing option is

$$u(x,\tau) = C\exp(-rT)N(d_1).$$

Table 2 lists the prices for the cash or nothing option, errors, and convergence rates calculated by the proposed method.

4. Discussion

In this section, we take the European call option as an example to compare the proposed ADE-based "no-far-field" method with the explicit Euler scheme under the same "no-far-field" framework. We then emphasize why the ADE approach is particularly well suited for stress-testing and real-time pricing applications. The standard forward-Euler discretization becomes unstable unless the time step Δt is chosen extremely small, on the order of

$$\Delta t \lesssim \frac{h^2}{\sigma^2 x_{\max}^2}.$$

By contrast, the ADE scheme maintains numerical stability for time steps up to an order of magnitude larger. In our code tests, the ADE method remains stable where Euler already exhibits large oscillations or outright blow-ups. Comparison of the two methods is displayed in Fig. 6(a), (b) and (c). Setting the time step to ten times the original, the ADE method still maintains good numerical solution stability. While allowing for larger time steps, the ADE method maintains second-order convergence, as listed in Tables 1 and 2.

Pricing of derivatives such as options is a core tool in financial risk management. If the underlying pricing model is unstable or computationally inefficient, it can lead to hedging failures, asset mismatches, and mispricing under stress conditions (Andersen and

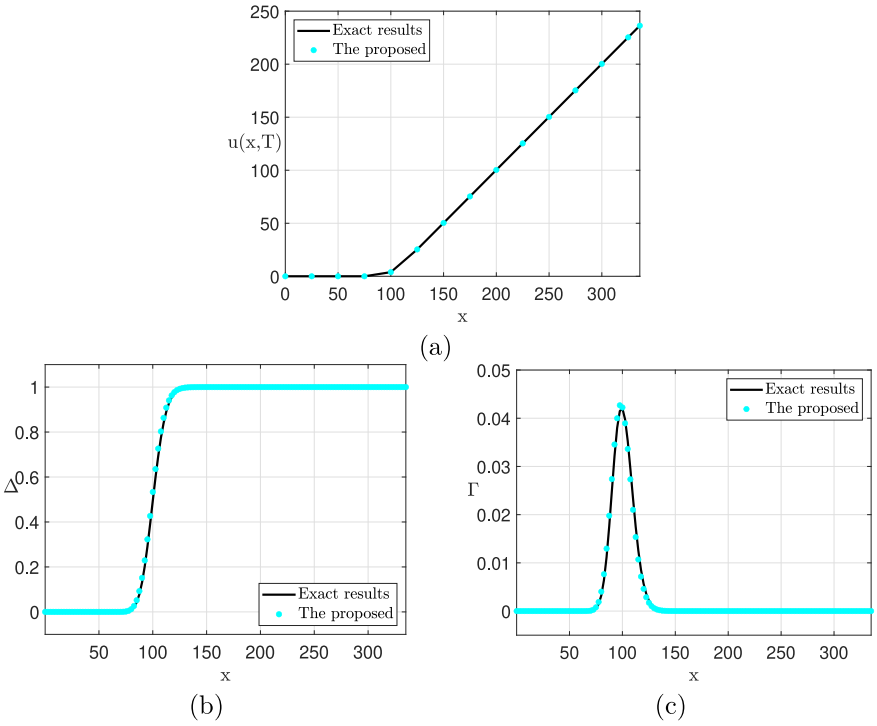

Fig. 5. (a) Numerical and exact prices of European call option, (b) Numerical and exact Δ of European call option, (c) Numerical and exact Γ of European call option.

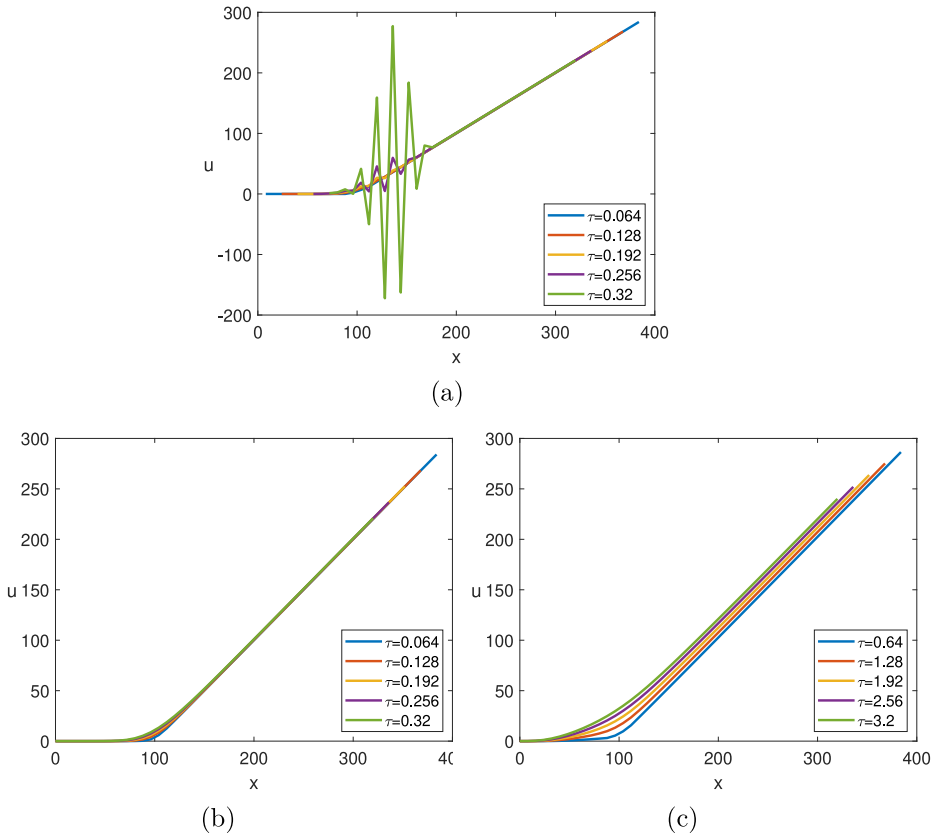

Fig. 6. (a) Numerical prices at $\Delta t = 0.032$(Explicit Euler method), (b) Numerical prices at $\Delta t = 0.032$(ADE method), (c) Numerical prices at $\Delta t = 0.32$(ADE method)

Table 2
Errors and convergence rates for the cash or nothing option at $x = 100$ with parameters $r = 0.03$, $\sigma = 0.3$, and $T = 0.1$. The exact value is 49.221.

N_τ	160	320	640	1280
Price	50.489	49.577	49.300	49.241
Error	1.2673	3.5569e−1	7.8509e−2	1.9144e−2
Convergence rate	1.83	2.18	2.04	

Table 3
The list of abbreviations.

Abbreviations	Full name
BS	Black–Scholes
ADE	Alternating Direction Explicit

Andreasen, 2000). Given that market shocks can propagate rapidly through derivative positions, robust and efficient numerical schemes are essential for maintaining pricing accuracy and systemic stability. In this context, our proposed ADE-based pricing scheme provides a numerically stable and computationally efficient alternative for real-time option valuation and stress-test simulations. Compared with traditional finite-difference schemes, it enables large time steps without compromising accuracy, which is critical for time-sensitive applications. Furthermore, derivatives have been shown to play a dual role in financial markets—enhancing efficiency and liquidity but also amplifying systemic linkages under stress (Sill, 1997; Bevilacqua et al., 2023; Li, 2021; Blanco and Wehrheim, 2017; Cao et al., 2024).

5. Conclusions

In this paper, we proposed a novel second-order FDM for solving the BS equation without far-field boundary conditions. The proposed numerical method is based on the ADE method, which allows large time steps while maintaining numerical stability. To improve computational efficiency, we used a methodology that does not require far-field boundary conditions. Furthermore, we applied a non-uniform grid to further improve computational efficiency. Computational results on European and cash-or-nothing options demonstrated the second-order convergence of the numerical scheme. This approach is particularly suitable for real-time financial applications where speed and robustness are critical, such as risk assessment and high-frequency pricing. Future research will focus on extending the method to higher-dimensional problems (e.g., basket options), incorporating adaptive mesh refinement, handling early-exercise features in American-style derivatives, and validating results using empirical market data.

List of abbreviations

See Table 3.

CRediT authorship contribution statement

Jian Wang: Writing – original draft, Data curation, Conceptualization. **Lin Wu:** Writing – original draft, Methodology, Investigation. **Xinpei Wu:** Writing – original draft, Methodology, Investigation. **Youngjin Hwang:** Software, Resources, Project administration. **Yunjae Nam:** Software, Resources, Methodology. **Soobin Kwak:** Validation, Supervision, Software. **Taehui Lee:** Methodology, Investigation. **Junseok Kim:** Writing – review & editing, Supervision, Resources, Project administration, Methodology.

Declaration of competing interest

The authors declare that they have no known competing financial interests or personal relationships that could have appeared to influence the work reported in this paper.

Acknowledgements

The corresponding author (J.S. Kim) was supported by Korea University Grant K2504591.

Appendix

MATLAB codes for the European call and cash or nothing options.

```
% 1D Black-Scholes equation without far-field boundary condition
clear; clc; format short e;
% Set the problem parameters
K = 100;              % Strike price
sig = 0.3;            % Volatility
r = 0.03;             % Risk-free interest rate
C = 100;              % Payout for the cash-or-nothing option
Smax = 4*K;           % Maximum asset price (domain upper bound)
S0 = 100;             % Initial asset price
T = 0.1;              % Maturity time
% Initialize the figure for plotting
figure(1); clf; hold on; box on; set(gca, 'FontSize', 12)
flag = 1;    % flag=1: call option, flag=2: cash-or-nothing option
h = 0.05;    % Spatial step size
% Generate spatial grid points
if flag == 1
    x = [0:h:Smax];  % Uniform grid for call option
else
    % Staggered grid for the cash-or-nothing option
    x = [0 0.5*h:h:Smax-0.5*h Smax];
end
% Compute spatial steps and number of grid points
h = diff(x); Nx = length(x);
% Loop over different time resolutions
for k = 1:4
    Nt = 80 * 2^k;      % Number of time steps
    dt = T / Nt;        % Time step size
    np = floor(Nt / 10); % Plotting interval
    % Initialize solution matrix
    U = nan(Nx, Nt+1);
    U(1, :) = 0;        % Boundary condition at x=0
    % Set initial condition (payoff function)
    for i = 1:Nx
        if x(i) > K
            if flag == 1
                U(i, 1) = x(i) - K;     % Call option payoff
            else
                U(i, 1) = C;            % Cash-or-nothing payoff
            end
        else
            U(i, 1) = 0;
        end
    end
    % Precompute coefficients for Crank-Nicolson method
    for i = 2:Nx-1
    fac1(i)=1/dt+((sig*x(i))^2-r*x(i)*h(i))/(h(i-1)*(h(i-1)+h(i)))+0.5*r;
    fac2(i)=1/dt+((sig*x(i))^2+r*x(i)*h(i-1))/(h(i)*(h(i-1)+h(i)))+0.5*r;
    end
    % Time-stepping loop
    for n = 1:Nt
% Forward sweep: compute U(:,n+1) using known values from time step n
        for i = 2:Nx-n
         U(i,n+1)=(U(i,n)/dt+(sig*x(i))^2*((U(i+1,n)-U(i,n))/ ...
```

```
        (h(i)*(h(i-1)+h(i)))+U(i-1,n+1)/(h(i-1)*(h(i-1)+h(i))))+ ...
        r*x(i)*(h(i-1)*(U(i+1,n)-U(i,n))/(h(i)*(h(i-1)+h(i))) - ...
        h(i)*U(i-1,n+1)/(h(i-1)*(h(i-1)+h(i))))-0.5*r*U(i,n))/fac1(i);
    end
    % Save the forward step result
    V = U(:,n+1);
    % Backward sweep: refine U(:,n+1) using implicit correction
    for i = Nx-n-1:-1:2
     U(i,n+1) = (U(i,n)/dt + ...
            (sig*x(i))^2 * (U(i+1,n+1)/(h(i)*(h(i-1)+h(i))) - ...
            (U(i,n) - U(i-1,n)) / (h(i-1)*(h(i-1)+h(i))) + ...
            r*x(i) * (h(i-1)*U(i+1,n+1)/(h(i)*(h(i-1)+h(i))) + ...
            h(i)*(U(i,n) - U(i-1,n)) / (h(i-1)*(h(i-1)+h(i))) - ...
            0.5*r*U(i,n)) / fac2(i);
    end
% Average the forward and backward results (Crank-Nicolson scheme)
    U(:,n+1) = (U(:,n+1) + V) / 2;
end
% Plot the final solution profile at the last computed time step
figure(1); hold on;
plot(x(1:Nx-n), U(1:Nx-n,n), 'b', 'linewidth', 2);
drawnow; ylim('tight')
% Optional: mesh plot of solution surface
figure(2); clf
mesh(x, linspace(0, T, Nt+1), U')
% Return to figure 1 for overlay plotting
figure(1)
% Compute the exact solution for comparison
d1 = (log(S0/K) + (r - sig^2/2)*T) / (sig*sqrt(T));
if flag == 1 % Call option (Black-Scholes formula)
    d2 = d1 - sig*sqrt(T);
    exact = S0 * normcdf(d1) - K * exp(-r*T) * normcdf(d2);
else
    % Cash-or-nothing option (digital call)
    exact = C * exp(-r*T) * normcdf(d1);
    grid on;
end
% Interpolate the numerical solution and compute error
W = [interp1(x(1:Nx-n), U(1:Nx-n,n+1), S0, 'pchip') exact];
err(k) = abs(diff(W));  % Absolute error at S = S0
end
% Compute convergence rates
for i = 1:length(err)-1
    rate(i) = log2(err(i)/err(i+1));
end
% Display error and convergence rate
err
rate
```

Data availability

Data will be made available on request.

References

Albanese, C., Jaimungal, S., Rubisov, D.H., 2003. A two-state jump model. Quant. Finance 3 (2), 145.

Andersen, L., Andreasen, J., 2000. Jump-diffusion processes: Volatility smile fitting and numerical methods for option pricing. Rev. Deriv. Res. 4, 231–262.

Bayliss, A., Turkel, E., 1982. Far field boundary conditions for compressible flows. J. Comput. Phys. 48 (2), 182–199.

Benninga, S., Wiener, Z., 1997. The binomial option pricing model. Math. Educ. Res. 6, 27–34.

Bevilacqua, M., Tunaru, R., Vioto, D., 2023. Options-based systemic risk, financial distress, and macroeconomic downturns. J. Financ. Mark. 65, 100834.

Black, F., Scholes, M., 1973. The pricing of options and corporate liabilities. J. Political Econ. 81 (3), 637–654.

Blanco, I., Wehrheim, D., 2017. The bright side of financial derivatives: Options trading and firm innovation. J. Financ. Econ. 125 (1), 99–119.

Buckova, Z., Ehrhardt, M., Günther, M., 2015. Alternating direction explicit methods for convection diffusion equations. Acta Math. Univ. Comen. 84 (2), 309–325.

Campbell, L.J., Yin, B., 2007. On the stability of alternating-direction explicit methods for advection-diffusion equations. Numer. Methods Partial Differential Equations 23 (6), 1429–1444.

Cao, J., Goyal, A., Ke, S., Zhan, X., 2024. Options trading and stock price informativeness. J. Financ. Quant. Anal. 59 (4), 1516–1540.

Colonius, T., Taira, K., 2008. A fast immersed boundary method using a nullspace approach and multi-domain far-field boundary conditions. Comput. Methods Appl. Mech. Engrg. 197 (25–28), 2131–2146.

Dubey, V.P., Kumar, R., Kumar, D., 2019. A reliable treatment of residual power series method for time-fractional Black–Scholes European option pricing equations. Phys. A 533, 122040.

Engquist, B., Halpern, L., 1988. Far field boundary conditions for computation over long time. Appl. Numer. Math. 4 (1), 21–45.

Farnoosh, R., Rezazadeh, H., Sobhani, A., Beheshti, M.H., 2016. A numerical method for discrete single barrier option pricing with time-dependent parameters. Comput. Econ. 48 (1), 131–145.

Feng, C., Tan, J., Jiang, Z., Chen, S., 2020. A generalized European option pricing model with risk management. Phys. A 545, 123797.

Gustafsson, B., 1988. Far-field boundary conditions for time-dependent hyperbolic systems. SIAM J. Sci. Stat. Comput. 9 (5), 812–828.

Hanh, T.T.H., Thanh, D.N.H., 2019. Finite-difference method for the Gamma equation on non-uniform grids. Vietnam. J. Sci. Technol. Eng. 61 (4), 3–8.

Jeong, D., Yoo, M., Kim, J., 2018. Finite difference method for the Black–Scholes equation without boundary conditions. Comput. Econ. 51 (4), 961–972.

Kangro, R., Nicolaides, R., 2000. Far field boundary conditions for Black–Scholes equations. SIAM J. Numer. Anal. 38 (4), 1357–1368.

Kim, S., Lyu, J., Lee, W., Park, E., Jang, H., Lee, C., Kim, J., 2024. A practical Monte Carlo method for pricing equity-linked securities with time-dependent volatility and interest rate. Comput. Econ. 63, 2069–2086.

Lee, C., Kwak, S., Hwang, Y., Kim, J., 2023. Accurate and efficient finite difference method for the Black–Scholes model with no far-field boundary conditions. Comput. Econ. 61, 1207–1224.

Li, K., 2021. The effect of option trading. Financ. Innov. 7 (1), 65.

Lyu, J., Park, E., Kim, S., Lee, W., Lee, C., Yoon, S., Park, J., Kim, J., 2021. Optimal non-uniform finite difference grids for the Black–Scholes equations. Math. Comput. Simulation 182, 690–704.

Ma, C., Ma, Z., Xiao, S., 2019. A closed-form pricing formula for vulnerable European options under stochastic yield spreads and interest rates. Chaos Solitons Fractals 123, 59–68.

Mashayekhi, S., Mousavi, S.N., 2022. A robust numerical method for single and multi-asset option pricing. AIMS Math. 7 (3), 3771–3787.

Pealat, G., Duffy, D.J., 2011. The alternating direction explicit (ADE) method for one-factor problems. Wilmott 2011 (54), 54–60.

Pourghanbar, S., Manafian, J., Ranjbar, M., Aliyeva, A., Gasimov, Y.S., 2020. An efficient alternating direction explicit method for solving a nonlinear partial differential equation. Math. Probl. Eng. 2020 (2020), 1–12.

Rendleman, R.J., 1979. Two-state option pricing. J. Financ. 34 (5), 1093–1110.

Saul'Yev, V.K., 1964. Integration of Equations of Parabolic Type By the Method of Nets. Pergamon.

Shen, J., Pretorius, F., 2013. Binomial option pricing models for real estate development. J. Prop. Invest. Financ. 31 (5), 418–440.

Sill, K., 1997. The economic benefits and risks of derivative securities. Bus. Rev. 1, 15–26.

Soleymani, F., Akgül, A., 2019. Improved numerical solution of multi-asset option pricing problem: A localized RBF-FD approach. Chaos Solitons Fractals 119, 298–309.

Sosa-Correa, W.O., Ramos, A.M., Vasconcelos, G.L., 2018. Investigation of non-Gaussian effects in the Brazilian option market. Phys. A 496, 525–539.

Svärd, M., Carpenter, M.H., Nordström, J., 2007. A stable high-order finite difference scheme for the compressible Navier–Stokes equations, far-field boundary conditions. J. Comput. Phys. 225 (1), 1020–1038.

Tian, Y.S., 1999. A flexible binomial option pricing model. J. Futures Mark.: Futures Options Other Deriv. Prod. 19 (7), 817–843.

Jian Wang received Ph.D. degrees in Applied Mathematics from Korea University, Korea, in 2020. He joined the School of Mathematics and Statistics, Nanjing University of Information Science and Technology, China in 2020. He is currently a professor at the Department of Information and Computing Science. His research interests include phase-field theory, fractal theory, and finance mathematics.

Lin Wu is a master's student studying in School of Mathematics and Statistics, Nanjing University of Information Science and Technology, China.

Xinpei Wu is a master's student studying in the Department of Mathematics at Korea University, Korea.

Youngjin Hwang is a Ph.D. student in the Department of Mathematics at Korea University, Korea. His research interests include phase-field, finite difference method, computational fluid dynamics, and mathematical modeling.

Yunjae Nam is graduate studying in Program in Actuarial Science and Financial Engineering, Korea University, Korea. And he received B.S. degree in Mathematic education, Incheon National University, Korea in 2024. His research interests are computational finance and portfolio optimization.

Soobin Kwak is a Ph.D. candidate at the Department of Mathematics, Korea University, Korea. And she received B.S. degree in Mathematics from Daegu University, Korea in 2020. Her research interests are phase-field, mathematical modeling, computational fluid dynamics, and scientific computing.

Taehui Lee is a master's student at the Program in Actuarial Science and Financial Engineering, Korea University, Korea. And he received B.S. degree in Mathematics from Korea University Sejong Campus, Korea in 2022. His research interest is in computational finance.

Junseok Kim received his Ph.D. in Applied Mathematics from the University of Minnesota, U.S.A. in 2002. He also received his B.S. degree from the Department of Mathematics Education, Korea University, Korea in 1995. He joined the faculty of Korea University, Korea in 2008 where he is currently a full professor at the Department of Mathematics. His research interests are in computational finance and computational fluid dynamics.